UC San Diego

UC San Diego Previously Published Works

Title

UTE imaging with simultaneous water and fat signal suppression using a time-efficient multispoke inversion recovery pulse sequence

Permalink

https://escholarship.org/uc/item/1678801h

Journal

Magnetic Resonance in Medicine, 76(2)

ISSN

0740-3194

Authors

Carl, Michael
Bydder, Graeme M
Du, Jiang

Publication Date

2016-08-01

DOI

10.1002/mrm.25823

Copyright Information

This work is made available under the terms of a Creative Commons Attribution License, availalbe at https://creativecommons.org/licenses/by/4.0/

Peer reviewed

eScholarship.org Powered by the California Digital Library
University of California

Author Manuscript

Author Manuscript

Author Manuscript

Author Manuscript

HHS Public Access

Author manuscript

Magn Reson Med. Author manuscript; available in PMC 2016 November 01.

Published in final edited form as:

Magn Reson Med. 2016 August ; 76(2): 577–582. doi:10.1002/mrm.25823.

UTE Imaging with Simultaneous Water and Fat Signal Suppression Using a Time-Efficient Multispoke Inversion Recovery Pulse Sequence

Michael Carl[1,*], **Graeme M. Bydder**[2], and **Jiang Du**[2]

[1]GE Healthcare, University of California, San Diego, California, USA

[2]Radiology Department, University of California, San Diego, California, USA

Abstract

Purpose—The long repetition time and inversion time with inversion recovery preparation ultrashort echo (UTE) often causes prohibitively long scan times. We present an optimized method for long T2 signal suppression in which several k-space spokes are acquired after each inversion preparation.

Theory and Methods—Using Bloch equations the sequence parameters such as TI and flip angle were optimized to suppress the long T2 fat and water signals and to maximize short T2 contrast. Volunteer imaging was performed on a healthy male volunteer. Inversion recovery preparation was performed using a Silver-Hoult adiabatic inversion pulses together with a three-dimensional (3D) UTE (3D Cones) acquisition.

Results—The theoretical signal curves generally agreed with the experimentally measured region of interest curves. The multispoke inversion recovery method showed good muscle and fatty bone marrow suppression, and highlighted short T2 signals such as these from the femoral and tibial cortex.

Conclusion—Inversion recovery 3D UTE imaging with multiple spoke acquisitions can be used to effectively suppress long T2 signals and highlight short T2 signals within clinical scan times. Theoretical modeling can be used to determine sequence parameters to optimize long T2 signal suppression and maximize short T2 signals. Experimental results on a volunteer confirmed the theoretical predictions.

Keywords

adiabatic inversion; ultrashort echo (UTE); T2 contrast; water and fat suppression

Introduction

Direct imaging of the very short T2 tissues which are frequently encountered in the musculoskeletal system when using MRI usually requires specialized pulse sequences with very short echo times (TEs). Ultrashort TE (UTE) sequences of this type typically acquire k-

*Correspondence to: Michael Carl, Ph.D., GE Healthcare, 408 Dickinson Street, San Diego, CA 92103-8226. michael.carl@ge.com.

Author Manuscript Author Manuscript Author Manuscript Author Manuscript

space data as soon as possible after the radiofrequency (RF) excitation in a center out manner (1). Often the native UTE images are mainly proton-density or T1-weighted and lack contrast between very short T2 (less than 1 ms) and longer T2 (greater than 10 ms) tissues. Several techniques such as dual echo subtraction or off-resonance saturation can be used to suppress longer T2 signals and highlight short T2 tissues in UTE imaging. Magnetization preparation with inversion recovery (IR) is another method available to generate contrast between short T2 tissues and longer T2 tissues. This is done by selectively reducing or eliminating long T2 signals in the image, such as those from fat, or water in muscle (2). Traditionally, with this approach one k-space spoke is acquired after each application of either a single or a dual inversion pulse (3). This can often be very scan time inefficient due to the large number of spokes that need to be collected in UTE imaging. In this work we explore the use of several k-space spokes after the application of a single inversion pulse to achieve longer T2 signal suppression (4–7) using a three-dimensional (3D) UTE (3D Cones) sequence. Theoretical calculations and simulations were used to optimize sequence parameters such as the inversion time (TI) and the flip angle (θ). Volunteer studies were then performed using this approach to demonstrate direct imaging of short T2 tissues such as cortical bone with long T2 suppression in clinically acceptable scan times.

Theory

Features of the pulse sequence used in this study are shown in Figure 1. The adiabatic inversion pulse is repeated every repetition time (TR) period, after which data from N separate k-space spokes is acquired. These are separated by equal time intervals τ (see Figure 1, lower, for an example with N = 5). TI is defined as the time from the center of the inversion pulse to the center-spoke of the acquisition, so that the sequence timing asymptotically approaches the conventional single spoke case for small values of N. To minimize scan time, TR is typically minimized based on specific absorption ratio (SAR) and other considerations.

By tracking the recursive steady state z-magnetization using the Bloch equations it is possible to derive an equation for the z-magnetization of spins with spin-density ρ available to be excited by the i^{th} excitation pulse with excitation flip angle θ, as shown in Eq. [1]. However, not all tissue magnetization is inverted by the inversion pulse. This can be accounted for by including a variable inversion efficiency factor Q, with a range of Q = –1 signifying full inversion to Q = 1 signifying no disturbance to the z-magnetization. Very short T2 tissues in the range between 100 μs and 2 ms are typically not inverted but are saturated by the adiabatic inversion pulse (8) (so that Q = 0). To simplify the signal equations, T2* decay during the UTE excitation pulses was not taken into account. Using this approach:

Author Manuscript Author Manuscript Author Manuscript Author Manuscript

$$M_i^z = \rho \left(\frac{[(1-E_W)E_P Q + (1-E_P) + (1-E_T)E_P E_W Q \sum_{j=1}^{N-1} (\cos(\theta))^j E_T^{(j-1)}]}{1-(\cos(\theta))^N E_T^{(N-1)} E_P E_W Q} (E_T \cos(\theta))^{(i-1)} + (1-E_T) \sum_{k=1}^{i-1} (E_T \cos(\theta))^{(k-1)} \right), \quad [1]$$

using the following definitions: $E_W \equiv e^{-\frac{(TR-TI-\tau(N-1)/2)}{T1}}$, $E_P \equiv e^{-\frac{(TI-\tau(N-1)/2)}{T1}}$, $E_\tau \equiv e^{-\frac{\tau}{T1}}$

Equation [1] can be simplified for the case of short T2 tissues by setting Q = 0 and generating the signal available from short T2 signals S_i, by multiplying Eq. [1] by sin(θ).

$$S_i = \rho \sin(\theta) \left((1-E_P)(E_T \cos(\theta))^{(i-1)} + (1-E_T) \sum_{k=1}^{i-1} (E_T \cos(\theta))^{(k-1)} \right). \quad [2]$$

Long T2 Signal Suppression

The most direct way to eliminate the signal from a tissue with a given value of T1 is to use a single UTE acquisition with TI corresponding to the null point. When several spokes near the null point are applied, signal suppression is still possible since excited signals before the null point are of opposite polarity to these acquired after the null point. These then cancel in the regridding process during image reconstruction. When several tissues with different T1s are present (such as fat and water in muscle), only one tissue can be accurately nulled. Because fat has a shorter T1 and a faster recovery rate than water in muscle, overall long-T2 signal suppression is best achieved by choosing the null point for fat signals. Because fat has a multicomponent spectrum (9), Eq. [1] can be used for each spectral peak separately and then summed to give the total fat signal.

At the null point for fat, the longitudinal magnetization of long T2 water in muscle or cortical bone pore water (10) has not yet reached its null point; however, its steady-state z-magnetization is low due to its relatively long T1 and the continuous inversion and re-inversion of its z-magnetization produced by the inversion pulses.

The magnetization of short T2 tissues within the cortical bone is not inverted, but instead is saturated by the adiabatic inversion pulse. It therefore recovers to a positive longitudinal magnetization during TI. Figure 2 shows the simulated evolution of the longitudinal magnetization as it approaches steady state for fat (red), muscle water (blue), and cortical bone (black). These simulation results were generated using TR = 50 ms, TI = 24 ms, and τ = 5 ms, with the number of excitations spokes per inversion pulse N = 5, and a flip angle of θ = 20° for each excitation pulse. For these and subsequent simulations we used the fat spectra for white adipose tissue from (9) resulting in average T1/T2 for fat of approximately

Author Manuscript Author Manuscript Author Manuscript Author Manuscript

300–350 ms/60 ms. The corresponding values used for water in muscle and bone were 1400 ms/35 ms and 300 ms/0.3 ms, respectively.

For relatively low flip angles, the z-magnetization recovery between inversion pulses is not significantly disturbed by the excitation pulses so that TI can simply be set to null fat (using an average value of T1 for fat of approximately 300–350 ms at 3 Tesla [T]) and is given by:

$$TI = -T_1 \ln\left(\frac{1+e^{-TR/T_1}}{2}\right). \quad [3]$$

For larger flip angles however, the z-magnetization gets driven toward zero. This tends to shorten the recovery time to the null point and, hence, the required TI.

Figure 2B shows a zoomed version of the steady state fat signal for both the z-magnetization and the xy-magnetization with similar sequence parameters to those used in Figure 2A. The case for lower flip angles (e.g., $\theta = 20°$) is shown in blue with a nominal nulling TI for fat of 24 ms. Here the z-magnetization is relatively undisturbed by the N = 5 excitation pulses and the xy-magnetization clusters symmetrically below and above zero, resulting in good overall fat suppression after regridding due to fat signal cancellation. However, for the case shown in red using higher flip angles (e.g., $\theta = 50°$) and the same nominal nulling TI of fat (24 ms) the z-magnetization shows more significant effects due to the higher flip angle excitation pulses as well as an effectively shortened null-time. More importantly, in this case the net xy-magnetization does not cancel and this causes incomplete fat signal suppression in the final image. To achieve better signal suppression for fat, the spokes can be acquired at a shorter value of TI as shown in black. The exact TI can be reliably calculated using Eq. [1] and yields TI = 20 ms for the sequence parameters used in Figure 2B. Note how the net xy-magnetization of the five spokes cancels as desired in this case resulting in well suppressed fat signal in the final image.

The dependence of the nulling time of fat on the flip angle and the number of spokes is shown in Figure 3A. As expected there is no dependence of the TI on flip angle for the conventional case of N = 1, because a single excitation at the null point does not affect the z-magnetization irrespective of the flip angle used. For N > 1, however, the TI to null fat is reduced at higher flip angles as already indicated in Figure 2B. For example, for N = 5 (black line) and excitation flip angle $\theta = 50°$, the optimum TI is 20 ms.

Short T2 Optimization

The considerations above were designed to optimize long T2 signal suppression. It is also possible to use Eq. [2] to determine the flip angle that maximizes short T2 signals. Setting the derivative of S_i in Eq. [2] with respect to θ to zero, and invoking the approximations that $\tau \ll T1$ and the flip angle is small, an approximate expression for optimizing the excitation flip angle θ can be derived:

Author Manuscript Author Manuscript Author Manuscript Author Manuscript

$$\theta \approx \sqrt{\frac{2N-1}{N^2 - N/2 - 1/4}} \approx \sqrt{\frac{2}{N}} \quad [4]$$

Figure 3B shows the theoretical (dotted lines) and simulated optimum flip angles (markers) as a function of the number of spokes (N) per inversion pulses. Three theoretical curves are shown: The dotted black line corresponds to the first part of Eq. [4], while the dotted cyan line corresponds to the second approximation in Eq. [4]. For reference, the dotted green line shows the results of the transcendental equation (not shown) from setting the derivative of S_i in Eq. [2] to zero, before the small tip angle approximation is invoked. For the simulations, two cases are displayed. The first, shown in blue are simulation results using a 300 μs duration hard excitation RF pulse (which may be needed to obtain higher flip angles on clinical scanners). To eliminate the effects of T2 decay during the RF pulse (which was not included in Eq. [1]) the red markers show the results using an instantaneous UTE excitation RF. As can be seen, the theoretical line using Eq. [4] agrees well with the simulation data points. The small underestimation from the simulated data shown in red is due to the small tip angle approximation, while the deviation from the blue data points stems from the T2 decay during the RF pulse in the simulated data. As expected, the more RF pulses that are applied between the inversion pulses (larger N), the lower the optimum flip angle becomes to conserve the z-magnetization across all N RF pulses. The conventional case of N = 1 yields an optimum flip angle value of 90° to maximize the short T2 signal.

Methods

Volunteer imaging was performed on a healthy male volunteer (age 70 years) using an eight-channel knee coil on a 3T GE HDxt clinical MR scanner. The 3D Cones sequence uses a unique k-sampling trajectory that samples data along twisting evenly spaced paths on cone surfaces in 3D (11). It samples data starting from the center of k-space and twists outward from there with the data acquisition starting as soon as possible after the RF excitation. Both RF and gradient spoiling are used to crush the remaining transverse magnetization after each data acquisition. Inversion preparation and excitation was performed using a 8.6 ms Silver-Hoult adiabatic inversion pulse (12) with a bandwidth of ∼1.5 kHz, and 300 μs duration hard excitation RF pulse, respectively. The TI was set to approximately the null point of fat at θ = 50°. Relevant sequence parameters were field of view (FOV) = 15 cm, matrix 256 × 256, slice thick = 5 mm, TE = 30 μs, TR = 50 ms, N = 5, τ = 5 ms, TI = 20 ms, and θ = 10° – 80°.

Further experiments were performed on the same volunteer (but during a separate scan session) to highlight the scan time savings that can be acquired using the multispoke approach. To minimize scan time, anisotropic FOV encoding together with slab-selection excitation was used to excite and encode only regions of interest. The slab selective RF pulse was a 600 μs minimum-phase Shinnar–Le Roux pulse with peak RF power near the end of the pulse. Using the same number of k-space spokes, several inversion prepared images were obtained using different values of N. Relevant sequence parameters were FOV = 15 cm, matrix 256 × 256, slice thick = 5 mm, 10 slices, TE = 30 μs, TR = 80 ms, τ = 5 ms, θ = 30°,

Author Manuscript Author Manuscript Author Manuscript Author Manuscript

and TI = optimum. SNR of the images was measured as the mean signal in a region of interest (ROI), divided by the standard deviation of the noise.

Results

Figure 4A shows several zoomed-in axial inversion recovery prepared 3D Cones images of the tibia. Using a TI of 20 ms, these shows good marrow signal suppression at $\theta = 50°$. For lower flip angles (e.g., $\theta = 10–40°$), the TI of 20 ms is too short to null marrow fat. As a result, a low signal transition band (arrow) is seen between the marrow (negative z-magnetization) and cortical bone (positive z-magnetization) similar to that seen with out-of-phase imaging using gradient echo sequences.

Figure 4B illustrates the scan time reductions achievable with the proposed techniques and sequence parameters. All images were sampled in k-space at the Nyquist criteria. Only odd numbers of spokes were used for these scans, however the technique also allows use of even values of N. With the total number of spokes (Nyquist) and TR fixed, the scan time scales as 1/N, meaning that the most significant scan time reduction can be achieved when switching from N = 1 to N = 3. For larger values of N, further increase yields smaller scan time savings. More importantly, as can be seen from Figure 4B, both SNR and overall image quality start to degrade. Overall we have observed the best results using N = 3–7. While the SNR predictably goes down for the shorter scans, the SNR efficiency (e.g., SNR normalized by scan-time) increases monotonically as a function of N.

Figure 5A shows the simulated signal curves using Eq. [1]. These generally agree with the experimentally measured ROI curves shown in Figure 5B, including the expected location of the minimum point for the fat signals. The overall signal amplitudes are arbitrary and depend on the (unknown) underlying spin density. The small deviation of the cortical bone signal maximum can be attributed to the rapid signal decay of the transverse magnetization of cortical bone, which has a short T2* ($\sim$300 μs) that is comparable to the excitation RF pulse duration (300 μs) used in our experiments. As was shown in (13–15) this leads to higher optimum flip angles.

Discussion

Although our experimental studies were mainly targeted at tissues with very short T2*s such as cortical bone (e.g., T2* < 1 ms), these methods may also be expanded to tissues such as menisci, tendons, and ligaments with intermediate short T2* (e.g., 2–8 ms). The longitudinal magnetization of such tissues only gets partially inverted and yields positive signal at the null point for fat. Further investigations will be needed to study the SNR efficiency for these applications compared with other long T2 suppression techniques such as dual echo subtraction.

The theoretical equations presented here can also be used to analyze the signal behavior of other types of preparation pulses, such as fat saturation, when they are used with multispoke UTE imaging. The multispectral nature of fat can be accurately modeled by using different values of Q for different peaks, e.g., Q = 0 for the peaks that are saturated by the spectrally

Author Manuscript Author Manuscript Author Manuscript Author Manuscript

selective fat saturation pulse, and Q = 1 for peaks near the main water peak that are not saturated. Work on this is in progress.

Limitations of the techniques include increased artifact levels with either larger values of N (see Figure 4B) or higher values of flip angle (see Figure 4A). Larger flip angles result in a greater asymmetry between the negative fat signals before the null-point and the positive fat signals after the null point (see Figure 2B lower). In addition, larger flip angles result in less uniform short T2 signals distributed amongst the N spokes (e.g., the first spoke may use up the majority of the longitudinal magnetization, leaving the subsequent spokes with less signal), resulting in larger fluctuations in signal between adjacent spokes. Finally, the desired cancellation of fat signals among the N spokes only functions if the spokes are close enough to their neighbors to offset one another during the regridding process. This may be compromised with large values of N unless the spoke-to-spoke sampling density is increased. While this was not studied in detail, it may also be possible to adjust the regridding kernel to optimize fat cancellation for larger values of N.

Conclusions

Inversion recovery 3D UTE imaging with multiple spoke acquisitions can be used to effectively suppress long T2 signals and highlight short T2 signals. The theoretical equations can be used to determine sequence parameters such as TI, and the excitation flip angle necessary to optimize long T2 signal suppression and maximize short T2 signals. In this optimization, a compromise has to be made between high SNR of very short T2 tissues such as cortical bone (which is achieved at higher flip angles) and sufficient long T2 suppression (which is best achieved at low to intermediate flip angles). In addition, very large flip angles often require relatively long RF pulse durations on clinical scanners relative to the very short T2 of tissues such as cortical bone. This also favors the use of low to intermediate flip angles. Volunteer scans showed excellent signal suppression efficiency for fat and long T2 muscle in clinical scan times of less than 5 min.

References

1. Rahmer J, Bornert P, Groen J, Bos C. Three-dimensional radial ultrashort echo-time imaging with T2 adapted sampling. Magn Reson Med. 2006; 55:1075–1082. [PubMed: 16538604]
2. Larson PE, Conolly SM, Pauly JM, Nishimura DG. Using adiabatic inversion pulses for long-T2 suppression in ultrashort echo time (UTE) imaging. Magn Reson Med. 2007; 58:952–961. [PubMed: 17969119]
3. Du J, Bydder M, Takahashi AM, Carl M, Chung CB, Bydder GM. Short T2 contrast with three-dimensional ultrashort echo time imaging. Magn Reson Imaging. 2011; 29:470–482. [PubMed: 21440400]
4. Zurek M, Johansson E, Risse F, Alamidi D, Olsson LE, Hockings PD. Accurate T1 mapping for oxygen-enhanced MRI in the mouse lung using a segmented inversion-recovery ultrashort echo-time sequence. Magn Reson Med. 2014; 71:2180–2185. [PubMed: 23878094]
5. Manhard MK, Horch RA, Harkins KD, Gochberg DF, Nyman JS, Does MD. Validation of quantitative bound- and pore-water imaging in cortical bone. Magn Reson Med. 2014; 71:2166–2171. [PubMed: 23878027]
6. Seifert AC, Li C, Rajapakse CS, Bashoor-Zadeh M, Bhagat YA, Wright AC, Zemel BS, Zavaliangos A, Wehrli FW. Bone mineral 31P and matrix bound water densities measured by solid state 31P and 1H MRI. NMR Biomed. 2014; 27:739–748. [PubMed: 24846186]

Author Manuscript Author Manuscript Author Manuscript Author Manuscript

7. Weiger M, Wu M, Wurnig MC, Kenkel D, Boss A, Andreisek G, Pruessmann KP. ZTE imaging with long-T2 suppression NMR Biomed. 2015; 28:247–254. [PubMed: 25521814]
8. Li C, Magland JF, Rad HS, Song HK, Wehrli FW. Comparison of optimized soft-tissue suppression schemes for ultrashort echo time MRI, Magn Reson Med. 2012; 68:680. [PubMed: 22161636]
9. Hamilton G, Smith DL Jr, Bydder M, Nayak KS, Hu HH. MR Properties of brown and white adipose tissues. J Magn Reson Imaging. 2011; 34:468–473. [PubMed: 21780237]
10. Li S, Ma L, Chang EY, Shao H, Chen J, Chung CB, Bydder GM, Du J. Effects of inversion time on inversion recovery prepared ultrashort echo time (IR-UTE) imaging of bound and pore water in cortical bone. NMR Biomed. 2015; 28:70–78. [PubMed: 25348196]
11. Gurney PT, Hargreaves BA, Nishimura DG. Design and analysis of a practical 3D cones trajectory. Magn Reson Med. 2006; 55:575–582. [PubMed: 16450366]
12. Silver MS, Joseph RI, Hoult DI. Highly selective $\pi/2$ and π pulse generation. J Magn Reson. 1984; 59:347–351.
13. Carl M, Bydder M, Du J, Takahashi A, Han E. Optimization of RF excitation to maximize signal and T2 contrast of tissues with rapid transverse relaxation. Magn Reson Med. 2010; 64:481–490. [PubMed: 20665792]
14. Springer F, Steidle G, Martirosian P, Claussen CD, Schick F. Effects of in-pulse transverse relaxation in 3D ultrashort echo time sequences: analytical derivation, comparison to numerical simulation and experimental application at 3T. J Magn Reson. 2010; 206:88–96. [PubMed: 20637661]
15. Carl M, Chiang JT, Du J. Maximizing MR signal for 2D UTE slice selection in the presence of rapid transverse relaxation. Magn Reson Imaging. 2014; 32:1006–1011. [PubMed: 24814323]

Author Manuscript Author Manuscript Author Manuscript Author Manuscript

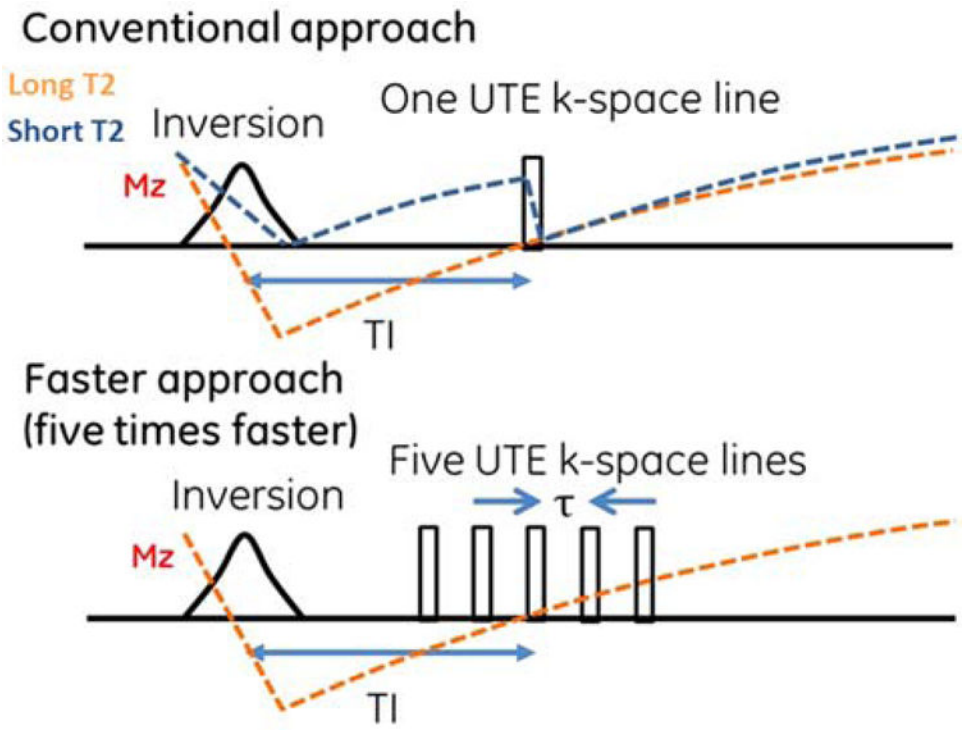

Fig. 1.

Diagram of inversion preparation and acquisitions used in conventional (upper) and faster (lower) UTE imaging approaches. Because five spokes are acquired during the faster approach, this results in a five-fold reduction in scan time for a given TR.

Author Manuscript Author Manuscript Author Manuscript Author Manuscript

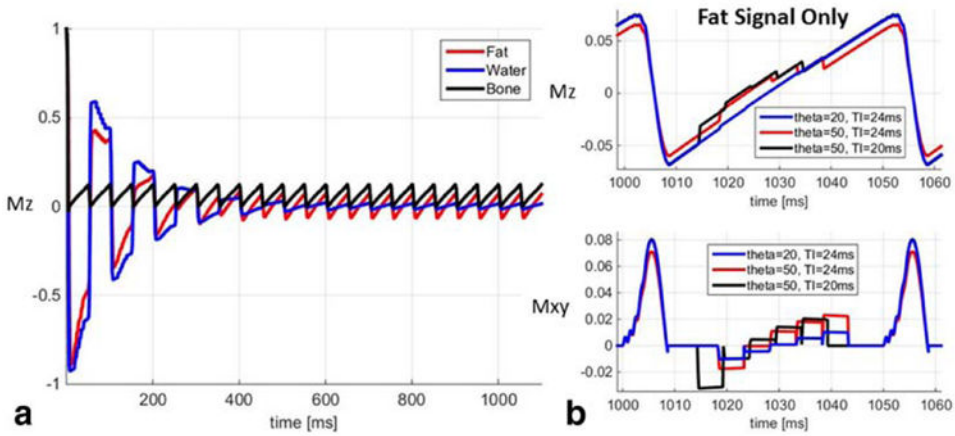

Fig. 2.

A: Approach to steady state of the longitudinal magnetization of fat, muscle water and cortical bone. Because of its shorter T1, fat signals have a higher steady state z-magnetization than muscle water signals. The short T2 signals of cortical bone are saturated and subsequently maintain a positive steady state signal. **B**: Upper: Steady state z-magnetization of fat for different values of TI and flip angles (theta). Lower: The corresponding steady state xy-magnetization. For lower flip angles (e.g., $\theta = 20°$), the appropriate null time can be calculated using Eq. [3]. For larger flip angles (e.g., $\theta = 50°$) however, a shorter TI (which can be calculated using Eq. [1]) is required.

Author Manuscript Author Manuscript Author Manuscript Author Manuscript

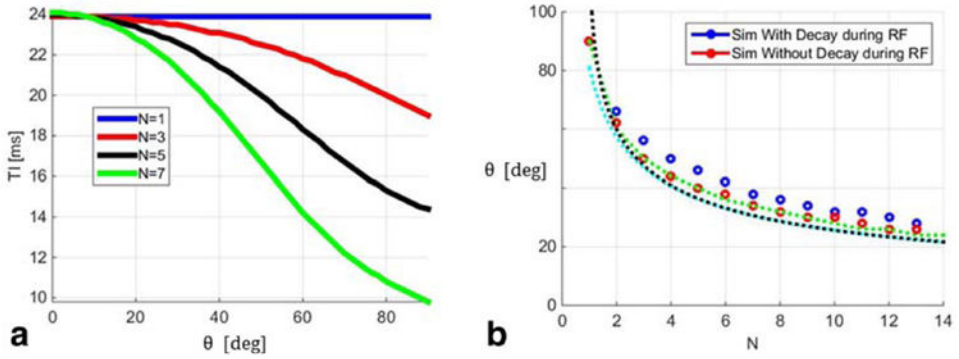

Fig. 3.

A: Dependence of the optimum TI on the flip angle (θ) for number of spokes (N) in the case where TR = 50 ms and τ = 5 ms. Generally, the optimum nulling TI is reduced for larger flip angles due to the z-magnetization being driven toward zero. For lower flip angles the optimum TI converges to the null time of fat irrespective on how many spokes are acquired during each TI. **B**: Theoretical and simulated optimum flip angles with and without decay during the RF pulses to maximize short T2 signals as a function of number of spokes N. Also shown are three theoretical curves: The dotted black line corresponds to the first part of Eq. [4], while the dotted cyan line corresponds to the second approximation in Eq. [4]. Finally, the dotted green line shows the results of the transcendental equation from setting the derivative of S_i in Eq. [2] to zero, before the small tip angle approximation is invoked. As expected, the optimum flip angle is reduced for higher values of N.

Author Manuscript Author Manuscript Author Manuscript Author Manuscript

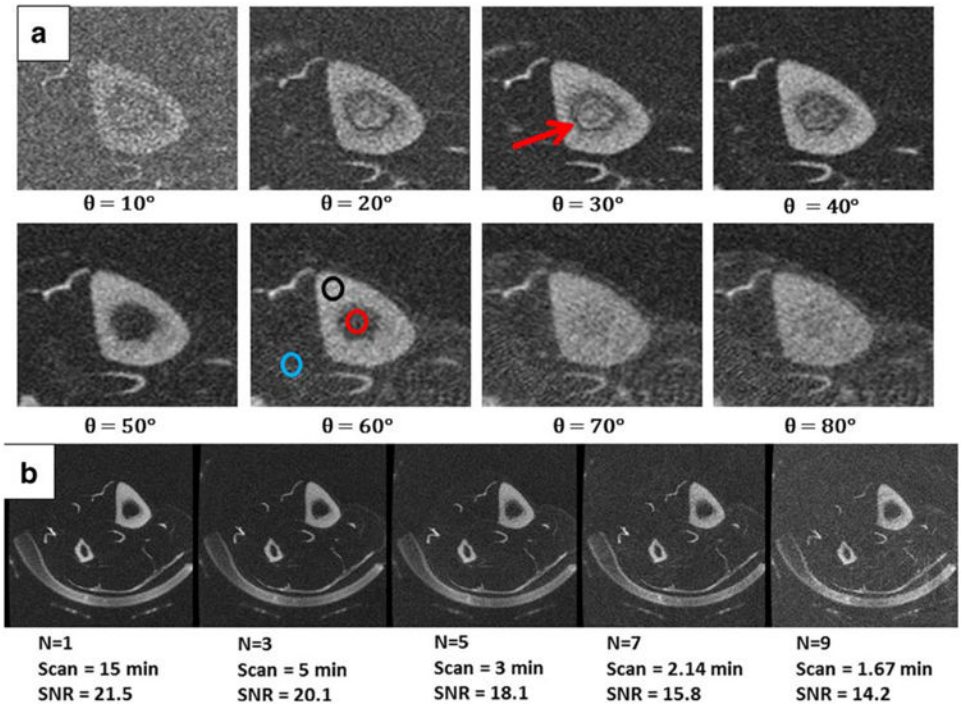

Fig. 4.

A: Axial tibial cortical bone images at various flip angles for TR = 50 ms, N = 5 and TI = 20 ms. Note the good central fatty bone marrow signal suppression at θ = 50°. For lower flip angles, a TI value of 20 ms is too early (see black line in Figure 3) and a low signal transition band between the marrow (negative z-magnetization) and cortical bone (positive z-magnetization) is seen (top row). This is similar to that seen with out-of-phase imaging using gradient echo sequences. **B**: Inversion prepared 3D Cones images (all sampled at the Nyquist limit) using different number of k-space spokes per inversion pulse. Note the significant scan time reduction when going from N = 1 to N = 3. Further increase in N yields smaller scan time benefits, and starts introducing some image artifacts.

Author Manuscript Author Manuscript Author Manuscript Author Manuscript

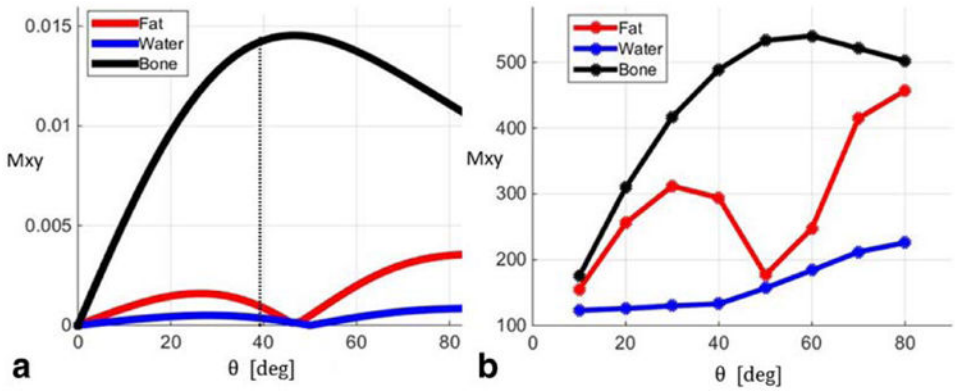

Fig. 5.

Simulated **(A)** and experimental **(B)** signals [a.u.] for marrow fat, water in muscle, and cortical bone. Also shown as a dashed line is the approximate theoretical flip angle to maximize short T2 cortical bone signal calculated using Eq. [4].